Accepted for IEEE International Symposium on Circuits and Systems ISCAS'99, May 30 – June 2, 1999, Orlando, FL.

AN FFT-BASED ALGORITHM FOR MULTICHANNEL BLIND DECONVOLUTION

Marcel Joho, Heinz Mathis, and George S. Moschytz

Signal and Information Processing Laboratory,
Swiss Federal Institute of Technology Zurich, Switzerland

joho@isi.ee.ethz.ch, tel.:+41 (0) 1 632 27 71, *mathis@isi.ee.ethz.ch, tel.:+41 (0) 1 632 36 20*, *moschytz@isi.ee.ethz.ch, tel.:+41 (0) 1 632 27 63*

ABSTRACT

A new update equation for the general multichannel blind deconvolution (MCBD) of a convolved mixture of source signals is derived. It is based on the update equation for blind source separation (BSS), which has been shown to be an alternative interpretation [1] of the natural gradient applied to the minimization of some mutual information criterion [2]. Computational complexity is held at a minimum by carrying out the separation/equalization task in the frequency domain. The algorithm is compared to similar known blind algorithms and its validity is demonstrated by simulations of real-world acoustic filters. In order to assess the performance of the algorithm, performance measures for multichannel blind deconvolution of signals are given in the paper.

1. INTRODUCTION

Blind separation, blind deconvolution and the combination of both, multichannel blind deconvolution, are tasks that have to be carried out in an increasing number of applications, particularly in acoustics and communications. The structure of the separation algorithm can be understood as a single-layer neural network, whose training algorithm and activation function depend partially on the statistics of the signals to be separated. Recently, training algorithms based on information-theoretic methods [3] or, more generally, higher-order statistics [4] have been used. Fast convergence can be achieved using the natural [2] or relative [5] gradient. In [1] a new update equation for the instantaneous mixing case has been derived, which is extended to the single- and multichannel deconvolution case in the course of this paper. In acoustics, long filters are usually required for the deconvolution process, which makes an implementation in the frequency domain advantageous. FFT-based algorithms for the deconvolution of one or more sources will therefore be derived and verified by simulations.

The measured signals $\mathbf{x} = [x_1, \ldots, x_M]^T$ to be processed are linear mixtures of the original source signals $\mathbf{s} = [s_1, \ldots, s_M]^T$ weighted by filters (convolution in the time domain)

$$\mathbf{x}(t) = (\mathbf{A} * \mathbf{s})(t) = \mathbf{A}(q)\mathbf{s}(t), \tag{1}$$

where M denotes the total number of sources and sensors. q and q^{-1} denote the forward shift and delay operator, respectively, e.g. $q^{-d}\mathbf{s}(t) = \mathbf{s}(t-d)$. $*$ is the convolution operator. Every element of the convolution mixing matrix $\mathbf{A}$ is a filter impulse response

$$[\mathbf{A}]_{lj} = \sum_k a_{ljk} q^{-k}, \tag{2}$$

representing the path from the jth source to the lth sensor. The dependency of the signals (but not of the mixing process) on the sampling time t is indicated in (1) but will be omitted in the following for better legibility.

2. BLIND SOURCE SEPARATION

If $a_{ljk} = 0$ for $k \neq 0$ in (2), multichannel blind deconvolution degenerates to the easier *blind source separation* (BSS) problem.

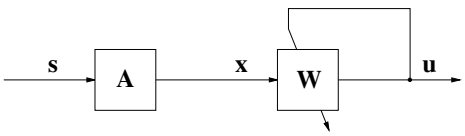

Figure 1: Blind source separation.

Fig. 1 shows the setup of a system for blind source separation. The source signals $\mathbf{s}$ are mixed by the mixing matrix $\mathbf{A}$ and recovery is attempted by a blind adaptive algorithm adjusting the coefficients of the separation matrix $\mathbf{W}$. The output of the algorithm is therefore

$$\mathbf{u} = [u_1, \ldots, u_M]^T = \mathbf{W}\mathbf{x} = \mathbf{W}\mathbf{A}\mathbf{s} = \mathbf{P}\mathbf{s}. \tag{3}$$

In order to separate the signals well, $\mathbf{WA} = \mathbf{P}$ should approximate as closely as possible a scaled permutation matrix. A possible update equation for the separation matrix $\mathbf{W}$ results from the minimization of the mutual information of the output signals [3] and applying the natural gradient [2]

$$\mathbf{W}_{t+1} = \mathbf{W}_t + \mu \left(\mathbf{I} - \mathbf{g}(\mathbf{u})\mathbf{u}^T\right)\mathbf{W}_t, \tag{4}$$

where μ is the step-size, $\mathbf{I}$ the identity matrix, and $\mathbf{g}(\mathbf{u})$ is known as the *Bussgang nonlinearity* [6]. *Blind* means that no components other than $\mathbf{x}$, $\mathbf{W}$ and $\mathbf{u}$ are involved in the update equation (4) or in the separation process $\mathbf{u} = \mathbf{W}\mathbf{x}$. A similar update equation to (4) has been derived in [1] through a different approach, which can be written for complex signals as

$$\mathbf{W}_{t+1} = \mathbf{W}_t + \mu \left(\mathbf{I} - \mathbf{g}(\mathbf{u})\mathbf{u}^H\right)\left[\mathbf{I} - \mu \left(\mathbf{I} - \mathbf{g}(\mathbf{u})\mathbf{u}^H\right)\right]^{-1}\mathbf{W}_t. \tag{5}$$

When $\mathbf{W}_t$ is close to the final solution $\mathbf{W}_\infty$, (5) converges to the natural gradient learning algorithm given by (4). Simulations have shown that the decorrelation process is slightly faster for (5) than for (4). Furthermore, (5) exhibits fewer outliers than (4) in the separation process for large step-sizes, and its variance of the separation performance measure is generally smaller for the same average separation.

Elimination of the matrix inversion in (5) can be accomplished by applying the *matrix inversion lemma*, in which case we obtain

$$\mathbf{W}_{t+1} = \mathbf{W}_t + \frac{\mu}{1-\mu}\left(\mathbf{I} - \frac{1}{1-\mu+\mu\mathbf{u}^H\mathbf{g}(\mathbf{u})}\mathbf{g}(\mathbf{u})\mathbf{u}^H\right)\mathbf{W}_t. \quad (6)$$

3. SINGLE-CHANNEL BLIND DECONVOLUTION

A much older problem than blind separation is *blind deconvolution* (BD) of a convolved signal

$$x(t) = (a * s)(t) = a(q)s(t), \quad (7)$$

where neither source signal $s(t)$ nor system impulse response $a(q)$ are known. Particularly in communications, when the channel impulse response is of no interest or is constantly changing, the problem is referred to as *blind equalization*. We will refer to this problem as single-channel blind deconvolution (SCBD) or simply blind deconvolution (BD). If (6) is adapted to deconvolve rather than separate, we get the update equation for the deconvolution filter $w(q) = \sum_k w_k q^{-k}$

$$w_{t+1}(q) = w_t(q) + \\ + \frac{\mu}{1-\mu}\left(1 - \frac{1}{1-\mu+\mu u_t^*(q)y_t(q)}y_t(q)u_t^*(q)\right)w_t(q), \quad (8)$$

where $u_t(q) = \sum_k u(t-k)q^{+k}$ and $y_t(q) = \sum_k g(u(t-k))q^{+k}$ represent the input to, and the output of the nonlinearity, respectively, The complex conjugate of $u_t(q)$ can be written as $u_t^*(q) = \sum_k u^*(t-k)q^{-k}$, implying time reversal. The z-transform of (8) is simply obtained by exchanging q with the z-operator. As z is replaced by $e^{j\omega T}$, the update equation can be evaluated at discrete frequencies in the frequency domain. Thus, transfering the signals

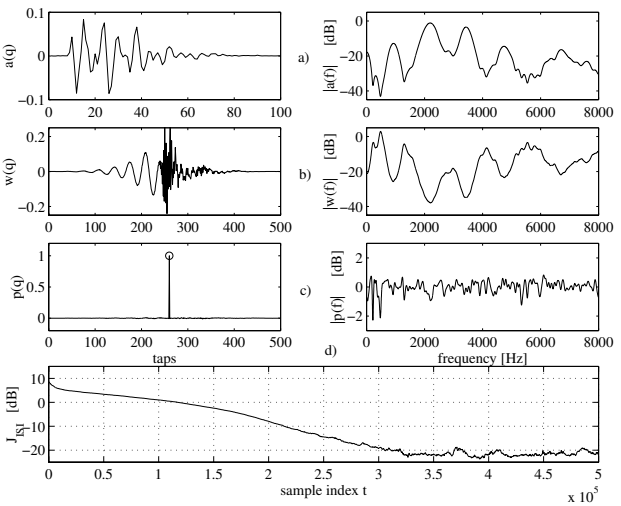

Figure 2: Single-channel blind deconvolution of an impulse response of a hearing aid feedback path. a) Measured impulse response $a(q)$ of feedback path and its spectrum. (dynamic range ≈ 40dB) b) Obtained impulse response $w(q)$ of inverse filter and its spectrum. c) Global response $p(q) = w(q)a(q)$ and its spectrum. d) Performance measure of blind deconvolution algorithm versus time.

into the frequency domain by an FFT, we get the update equation for the deconvolution filter $\tilde{\mathbf{w}}$ in the frequency domain

$$\tilde{\mathbf{w}}_{k+1} = \tilde{\mathbf{w}}_k + \\ + \frac{\mu}{1-\mu}\left(\mathbf{1} - \left((1-\mu)\mathbf{1} + \mu\tilde{\mathbf{u}}_k^* \odot \tilde{\mathbf{y}}_k\right)^{((-1))} \odot \tilde{\mathbf{y}}_k \odot \tilde{\mathbf{u}}_k^*\right) \odot \tilde{\mathbf{w}}_k, \quad (9)$$

with $\mathbf{1}$ being a vector of ones, k the block index, $\odot$ denoting the element-wise multiplication of two vectors, $\tilde{(.)}$ a vector in the frequency domain, and $(.)^{((-1))}$ the element-wise inversion of a vector or a matrix. Note that the nonlinearity is applied to the time series representation of the output signal $\tilde{\mathbf{y}}_k = \mathbf{Fg}(\mathbf{F}^{-1}\tilde{\mathbf{u}}_k)$, where $\mathbf{F}$ is the DFT matrix.

For the demonstration of the efficacy of the update equation shown above, we have taken a measured impulse response of the feedback path of a hearing aid as depicted in Fig. 2a). The first 100 taps have been used to filter gamma-distributed white noise, which we then try to blindly deconvolve using (9). Fig. 2b) shows the inverse filter the algorithm comes up with. In Fig. 2c) the convolution of the filter impulse response with the inverse filter impulse response illustrates the deconvolution performance. The location of the pulse can be controlled by the initial deconvolution filter $\tilde{\mathbf{w}}_0$. The filter length N of the adaptive inverse filter has to be chosen much longer than the original impulse response and satisfactory results have been obtained using $N = 500$ taps. The FFT length used is 1024, and the block length of the adaptation process is $L = 32$.

4. PERFORMANCE MEASURES

In order to find meaningful measures to judge the separation/deconvolution progress during convergence, scalar numbers are needed that describe the average degree of residual mixing, convolution, or a combination thereof, of the separated and deconvolved sources at the output of the network.

4.1. Blind Source Separation

Ideally, the scaled permutation matrix $\mathbf{P}$ in (3) would have one non-zero entry in each row i ($\mathbf{P}$ may happen to be diagonal dominant). p_{ij}^2 is the power transfer from source j to the output i. In each row i there will be one dominant entry ($\max_j p_{ij}^2$), indicating the power transfer of the separated source j. The other entries of the same row i of $\mathbf{P}$, which end up being non-zero in a realistic case, if squared and summed, reveal the power of other sources leaking through to the particular output i, if all sources have equal power. Vice versa, by squaring the subdominant entries of the same column of $\mathbf{P}$, we get the power of one source leaking through to different outputs. Provided the same-source lock-on is not a problem for the algorithm under consideration [7], the row-wise observation of the permutation matrix is more meaningful than the column-wise observation, rendering the performance index into a measure of *interchannel interference* (ICI) [1]

$$J_{\mathrm{ICI}}(\mathbf{P}) = \frac{1}{M}\sum_{i=1}^{M}\frac{\sum_{j=1}^{M} p_{ij}^2 - \max_j p_{ij}^2}{\max_j p_{ij}^2} = \frac{1}{M}\left(\sum_{i=1}^{M}\frac{\sum_{j=1}^{M} p_{ij}^2}{\max_j p_{ij}^2}\right) - 1. \quad (10)$$

Of course, $J_{\mathrm{ICI}}(\mathbf{P})$ is available in a simulation environment only. In practical situations, the true matrix $\mathbf{A}$ and therefore the matrix $\mathbf{P}$ are unknown.

4.2. Blind Deconvolution

In the BD case, the performance measure should reflect the deconvolution capability, hence indicating to what extent the deconvolved signal is influenced by adjacent samples of the same signal (convolutive noise). We define the overall system response as

$$p(q) = w(q)a(q) = \sum_{k=0}^{N_p} p_k q^{-k}, \tag{11}$$

where N_p is the order of the global FIR filter. Similarly to (10), the *intersymbol interference* (ISI) can be defined as

$$J_{\text{ISI}}(p(q)) = \frac{\sum_{k=0}^{N_p} p_k^2 - \max_k p_k^2}{\max_k p_k^2} = \frac{\sum_{k=0}^{N_p} p_k^2}{\max_k p_k^2} - 1. \tag{12}$$

4.3. Multichannel Blind Deconvolution

For the more general MCBD case, we are interested in both measures (10) and (12). We denote $\mathbf{P}(q)$ as the matrix of filter polynomials in q of the global system response with entries $[\mathbf{P}(q)]_{ij} = p_{ij}(q) = \sum_{k=0}^{N_p} p_{ijk} q^{-k}$ being the global filter response between source j and output i. Then we can find the averaged ICI as

$$J_{\text{ICI}}(\mathbf{P}(q)) = \frac{1}{M} \sum_{i=1}^{M} \frac{\sum_{j=1}^{M} \sum_{k=0}^{N_p} p_{ijk}^2}{\max_j \sum_{k=0}^{N_p} p_{ijk}^2} - 1. \tag{13}$$

J_{ICI} is also a meaningful measure for algorithms which only separate the source signals but do not attempt to deconvolve them.
For the calculation of the averaged ISI, each row of the permutation matrix is searched for the entry containing the filter with the most energy. By calculating the ISI of these entries and averaging over all rows, we get

$$J_{\text{ISI}}(\mathbf{P}(q)) = \frac{1}{M} \sum_{i=1}^{M} \frac{\sum_{k=0}^{N_p} p_{i,(\arg\max_j \sum_k p_{ijk}^2),k}^2}{\max_k p_{i,(\arg\max_j \sum_k p_{ijk}^2),k}^2} - 1. \tag{14}$$

An alternative measure reflecting both averaged ISI and ICI was defined in [7]

$$J_{\text{MC-ISI}}(\mathbf{P}(q)) = \frac{1}{M} \sum_{i=1}^{M} \frac{\sum_{j=1}^{M} \sum_{k=0}^{N_p} p_{ijk}^2}{\max_{j,k} p_{ijk}^2} - 1. \tag{15}$$

If (13) and (14) are only calculated row-wise, rather than averaged over all rows, a simple relationship between them and (15) can be found

$$J_{\text{MC-ISI}_{\text{row}}} = J_{\text{ICI}_{\text{row}}} + J_{\text{ISI}_{\text{row}}} + J_{\text{ICI}_{\text{row}}} \cdot J_{\text{ISI}_{\text{row}}}. \tag{16}$$

If $J_{\text{ICI}_{\text{row}}}$ and $J_{\text{ISI}_{\text{row}}}$ are small (good separation and deconvolution), $J_{\text{MC-ISI}_{\text{row}}}$ is roughly equal to the sum of these two measures. The corresponding results are obtained for a column-wise analysis.

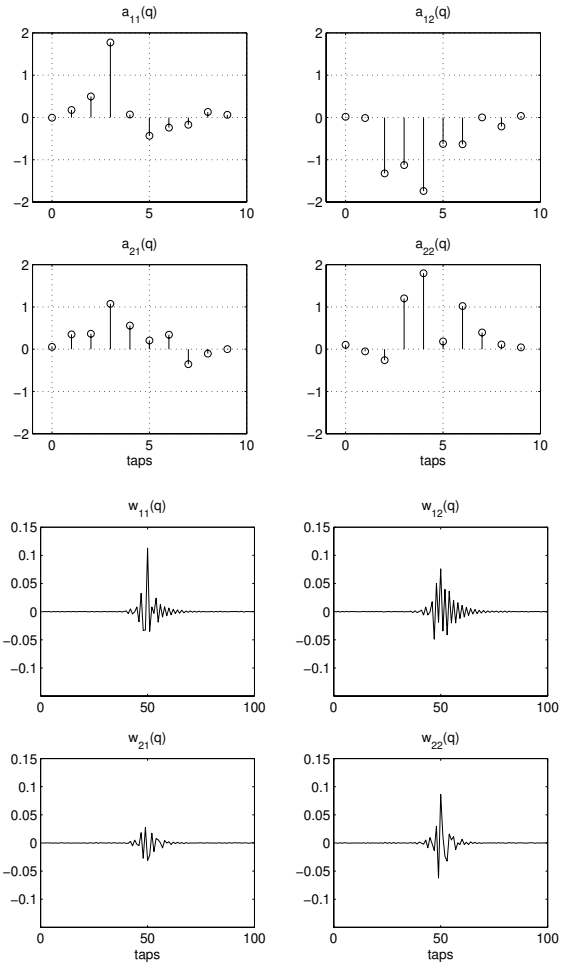

Figure 3: Multichannel blind deconvolution of two filtered sources. The upper four plots show the different randomly chosen, windowed filter impulse responses $a_{lj}(q)$ between source j and sensor l, while the lower four plots show the obtained impulse responses of the deconvolution filters $w_{il}(q)$ between sensor l and output i.

5. MULTICHANNEL BLIND DECONVOLUTION

In the real world, the problems of blind deconvolution and blind separation often have to be considered together. This is referred to as *multichannel blind deconvolution* (MCBD). MCBD can be either approached from the BSS side by replacing the scalars in the matrices by filter polynomials or from the BD side by replacing the single filter polynomial by a matrix of filter polynomials. Merging the two equations (6) and (8) and borrowing the *FIR matrix algebra* notations from [8] we get

$$\underline{\mathbf{W}}_{k+1} = \underline{\mathbf{W}}_k + \frac{\mu}{1-\mu} \left(\underline{\mathbf{I}} - \left((1-\mu)\underline{1} + \mu \underline{\mathbf{u}}_k^H \underline{\mathbf{y}}_k \right)^{-1} \underline{\mathbf{y}}_k \underline{\mathbf{u}}_k^H \right) \underline{\mathbf{W}}_k. \tag{17}$$

$\underline{(.)}$ denotes an FIR matrix or vector [8], whose elements are filter vectors in the frequency domain, e.g. $[\underline{\mathbf{W}}]_{il} = \tilde{\mathbf{w}}_{il}$. $\underline{1}$ is a 1×1 FIR matrix containing all ones, i.e. $[1 \ldots 1]$, and $\underline{\mathbf{I}} = \text{diag}(\underline{1}, \ldots, \underline{1})$.

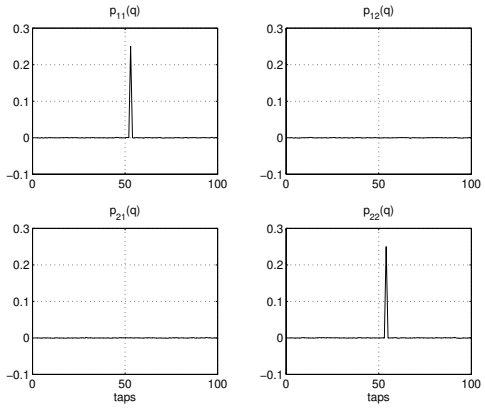

Figure 4: Multichannel blind deconvolution of two filtered sources. The four plots show the elements of $\mathbf{P}(q) = \mathbf{W}(q)\mathbf{A}(q)$, where $p_{ij}(q)$ is the impulse response between source j and output i. Notice for the desired channels we approximately get a delayed impulse, while for the cross-channels we get impulse responses close to zero, demonstrating the deconvolution and the separation capability, respectively.

A simulation of two filtered gamma-distributed sources has been carried out. The block length of the adaptive algorithm is $L = 16$ and the FFT length is 128. The impulse responses of the mixing channels and the obtained deconvolution filters (with $N = 100$ taps and the center tap in the middle) are shown in Fig. 3, and the resulting overall impulse responses $\mathbf{P}(q) = \mathbf{W}(q)\mathbf{A}(q)$ after MCBD are depicted in Fig. 4. For a good separation and deconvolution $\mathbf{P}(q)$ should come close to a permutation matrix, such that each row and column contains one dominant element close to a simple time delay q^{-d_i}, whereas the other elements approach zero. Performance curves are shown in Fig. 5. For the step-size chosen ($\mu = 0.001$), the separation process converges on a similar time-scale as the deconvolution process, leading to the fastest overall convergence. It has been observed, that for larger and smaller step-sizes, both convergence times increase, with the slower process being separation for smaller step-sizes, and deconvolution for larger step-sizes, respectively. An interesting property is that $J_{\text{ICI}}(\infty)$ and $J_{\text{ISI}}(\infty)$ converge to the same values. Furthermore, as the last term in (16)

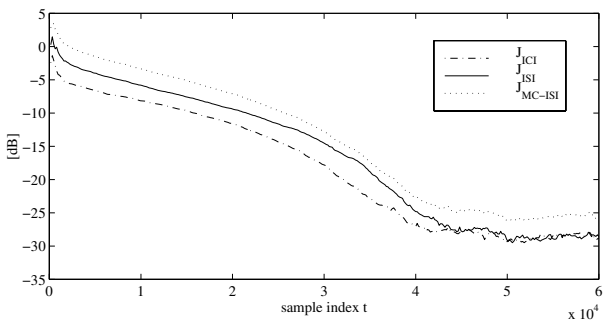

Figure 5: Performance measures for multichannel blind deconvolution of two filtered sources: Separation performance measure J_{ICI}, deconvolution performance measure J_{ISI}, and separation performance measure $J_{\text{MC-ISI}}$, as described above.

can be neglected for small values, $J_{\text{MC-ISI}}(\infty)$ is 3 dB higher than $J_{\text{ICI}}(\infty)$ and $J_{\text{ISI}}(\infty)$. Note that the delays of the different channel pulses might differ according to the delay indeterminacy of blind deconvolution. Because this task is much harder than either of the previously mentioned ones, convergence times are larger if compared with SCBD of similar filter lengths, or BSS of a similar number of sources. Other suitable update equations for FFT-based implementations of multichannel blind source separation can be found in [6, 8].

6. CONCLUSIONS

A modified update equation for blind source separation without any matrix inversion has been derived, which is of particular interest to the multichannel case. The update equation can be adapted to solve the single-channel blind deconvolution and the multichannel blind deconvolution problem, respectively. Since even relatively short impulse responses of real-world filters result in long inverse filters, separation and deconvolution algorithms operating in the frequency domain are advantageous. Efficient implementation of either algorithm can be realized in the frequency domain using overlap-save or overlap-add techniques, similarly to [9]. Performance measures introduced in the paper have shown the efficacy of the algorithms proposed.

7. REFERENCES

[1] M. Joho and H. Mathis, "Performance comparison of combined blind/non-blind source separation algorithms," in *Proc. First International Conference on Independent Component Analysis and Blind Source Separation ICA'99*, Aussois, France, January 11–15, 1999, pp. 139–142.

[2] S. Amari, A. Cichocki, and H. H. Yang, "A new learning algorithm for blind signal separation," *Advances in Neural Information Processing Systems*, vol. 8, pp. 752–763, 1996.

[3] A.J. Bell and T.J. Sejnowski, "An information-maximization approach to blind separation and blind deconvolution," *Neural Computation*, vol. 7, pp. 1129–1159, 1995.

[4] T-W. Lee, M. Girolami, A.J. Bell, and T.J. Sejnowski, "A unifying information-theoretic framework for independent component analysis," *International Journal on Mathematical and Computer Modeling*, in press, 1999.

[5] J.-F. Cardoso and B. Laheld, "Equivariant adaptive source separation," *IEEE Trans. on Sig. Proc.*, vol. 44, no. 12, pp. 3017–3030, Dec. 1996.

[6] R.H. Lambert and A.J. Bell, "Blind separation of multiple speakers in a multipath environment," in *International Conference on Acoustics, Speech & Signal Processing*, Munich, Germany, April 21–24, 1997, pp. 423–426.

[7] R. H. Lambert, "Difficulty measures and figures of merit for source separation," in *Proc. First International Conference on Independent Component Analysis and Blind Source Separation ICA'99*, Aussois, France, January 11–15, 1999, pp. 133–138.

[8] R.H. Lambert, *Multichannel Blind Deconvolution: FIR Matrix Algebra and Separation of Multipath Mixtures*, Ph.D. thesis, University of Southern California, 1996.

[9] E.R. Ferrara, "Fast implementations of LMS adaptive filters," *IEEE Transactions on Acoustics, Speech, and Signal Processing*, vol. ASSP-28, no. 4, pp. 474–475, 1980.